Enhancing Piezoelectric Properties of Bacterial Cellulose Films by Incorporation of $MnFe_2O_4$ Nanoparticles

Nipaporn Sriplai[1], Rahul Mangayil[2], Arno Pammo[3], Ville Santala[2], Sampo Tuukkanen[3], Supree Pinitsoontorn[1, 4,*]

[1]Materials Science and Nanotechnology Program, Department of Physics, Faculty of Science, Khon Kaen University, Khon Kaen 40002, THAILAND
[2]Faculty of Engineering and Natural Sciences (ENS), Tampere University (TAU), Tampere FI-33101, FINLAND
[3]Faculty of Medicine and Health Technology (MET), Tampere University (TAU), Tampere FI-33101, FINLAND
[4]Institute of Nanomaterials Research and Innovation for Energy (IN-RIE), NANOTEC- KKU RNN on Nanomaterials Research and Innovation for Energy, Khon Kaen University, Khon Kaen 40002, THAILAND

Abstract

Low-cost and highly sensitive piezoelectric sensors were fabricated from bacterial cellulose (BC) nanocomposite films. BC pellicles were biosynthesized using the bacterial strain, *Komagataeibacter xylinus*. BC/$MnFe_2O_4$ (MBC) nanocomposite films were fabricated via a co-precipitation method using manganese and iron ions in the presence of BC hydrogel, followed by hot-pressing. The films were characterized using a combination of scanning electron microscopy (SEM), transmission electron microscopy (TEM), X-ray diffraction (XRD), and atomic force microscopy (AFM) techniques. $MnFe_2O_4$ nanoparticles were found to impregnate the BC structure with a homogeneous distribution. The piezoelectric sensitivity measurements in the normal mode showed that the pristine BC film exhibited a sensitivity of about 5 pC/N, whereas this value was increased to 23 pC/N for the composite film, which is comparable to the polyvinylidene difluoride (PVDF) reference film. In the bending mode, the piezoelectric response increased to 25 pC/N and 57 pC/N for the BC film and the composite film, respectively. Moreover, the piezoelectric sensitivity was significantly enhanced using carbon tape electrodes attached directly to the films instead of sandwiched electrodes. This produced a sensitivity of greater than 50 pC/N for the MBC nanocomposite film in the normal mode measurement. Additionally, the studied sensors showed an almost linear increase of charge output with increasing dynamic force. This was particularly true for the MBC sensor. It showed a very high sensitivity of 80 pC/N with an applied force of 5 N. Our work demonstrates the potential of using MBC composite films as inexpensive and highly sensitive flexible piezoelectric sensors.

Keywords: bacterial cellulose; piezoelectric; sensor; composite; $MnFe_2O_4$;

*Corresponding author's e-mail address: psupree@kku.ac.th

1. Introduction

The piezoelectric effect is a phenomenon in which mechanical force is coverted into electrical energy [1]. It has helped enable development of smart systems and structures [2], as well as sensor applications [3]. For instance, the shivering of small animals in a metabolic study has been measured using the piezoelectric effect [4]. It was also exploited in a study of an insect-mimicking flapping-wing system for a modern flight innovation [5]. In medical applications, piezoelectric properties were used for medical imaging applications [6], sensors for blood pressure measurements [7], and acoustic nanosensors for biomimetic artificial hair cells [8].

Lightweight and flexible piezoelectric materials have been of great interest recently and have been applied in various fields, such as sensors, transducers, and actuators [9-11]. Several studies have focused on the use of polyvinylidene fluoride (PVDF) and its copolymers because of their high dielectric constant, high electroactive response, strong electrical dipole moment, high flexibility, high elastic modulus, and transparency [12-14]. However, the limitations of PVDF include its high cost, lack of sustainabity, and it is not biodegradable [15-17]. Piezoelectrics made from bio-based and renewable materials are now of great interest. Mangayil et al. fabricated low cost and flexible piezoelectric sensors produced from a bacterial cellulose (BC) film [15]. This film showed a piezoelectric response of 5-15 pC/N. The sensor charge increased as a function of increasing applied force in a manner similar to PVDF. This suggests BC may be applicable for sensor applications. BC sensors were very reliable during durability tests under sinusoidal load cycles for 1 h [15].

Very few studies related to the piezoelectric properties of BC have been reported. Pirich et al. prepared a dengue detection material by coating thin BC films on the surfaces of commercial piezoelectric sensors [18]. Their design provided ease of use, affordability and practical use for clinical diagnostics [18]. Furthermore, Zhang et al. fabricated vanadium doped ZnO microflowers in a BC matrix as a self-powered motion sensor [19]. The developed device can recognize forward and backward page-turning motions. This may lead to advances in the development of self-powered sensor networks, wearable electronics, and ambient intelligence applications [19]. Additionally, BC is flexible and lightweight, making it suitable for use in numerous electronic devices. Therefore, BC is a potential candidate material for flexible piezoelectric sensors.

On the other hand, manganese ferrite ($MnFe_2O_4$) nanoparticles are one of the important ferrite materials with interesting electrical and magnetic properties and potential applications in various fields. It has been studied for medical applications such as hyperthermia [20],

targeted drug delivery and magnetic resonance imaging [21]. In energy storage applications, $MnFe_2O_4$ nanoparticles were used as electrodes for supercapacitors [22] and as an anode for lithium-ion batteries [23]. Additionally, inclusion of $MnFe_2O_4$ in perovskite $BaTiO_3$ resulted in an increased piezoelectric coefficient (d_{33}) due to a lattice strain from unit cell distortion and lattice mismatch [24]. However, there have been no reports of piezoelectric sensitivity of composite materials containing BC and $MnFe_2O_4$ nanoparticles.

In this work, we fabricate and characterize a novel piezoelectric nanocomposite of BC and $MnFe_2O_4$ nanoparticles. The cellulose/$MnFe_2O_4$ system was reported in the literature for its magnetic behavior [25-27]. The synthesis processes detailed in the literature is complicated and requires special tools. In one route, Mn and Fe precursors along with other chemicals (hexadecanediol, dodecylamine, and dodecanoic acid) were dissolved in benzyl ether [25]. The mixture was heated to relatively high temperatures (140 - 300 °C), enabling chemical reactions to occur. In other research, $MnFe_2O_4$ nanoparticles were synthesized in the presence of cellulose at relatively lower temperatures (90 - 120 °C), but extra ultrasonication and a hydrothermal technique were required [26, 27]. In the present work, we used a much simpler synthesis process at relatively low temperature (65 °C) with no special tools. Moreover, our simple method produced a homogenous dispersion of $MnFe_2O_4$ nanoparticles throughout the samples.

The study of the BC/$MnFe_2O_4$ system for its piezoelectric response has never been reported. $MnFe_2O_4$ was chosen instead of other binary metal oxides, such as iron oxides, or manganese oxides, because of the stability of its spinel phase. Iron oxides are well known for their hydration reaction in humid environments, whereas manganese oxides can exist in various forms (Mn_2O_3, α-MnO_2, β-MnO_2, γ-MnO_2) in alkaline solutions [28]. Moreover, spinel $MnFe_2O_4$ consists of Mn^{2+} and Fe^{3+} ions distributed at both octahedral and tetrahedral sites [29], which could have an effect on electrostatic interactions between the $MnFe_2O_4$ nanoparticles and BC nanofibers.

Incorporating $MnFe_2O_4$ nanoparticles into a BC structure showed an enhancement in the piezoelectric sensitivity in normal force mode over that of pristine BC film. Additionally, we studied the piezoelectric response in a bending mode using a polydimethylsiloxane (PDMS) ring as a support, and also compared various electrode materials. The maximum piezoelectric value for the flexible BC/$MnFe_2O_4$ membrane was found to be more than 50 pC/N.

2. Materials and Methods

2.1 Chemicals

Yeast extract (LAB M), D-glucose (dextrose) anhydrous (AMRESCO, biotechnology grade), sodium hydroxide (NaOH, 99%, RCI Labscan), cellulase (≥700 units/g, Sigma-Aldrich), iron(III) chloride hexahydrate ($FeCl_3.6H_2O$, reagent grade, Sigma-Aldrich), manganese(II) chloride tetrahydrate ($MnCl_2.4H_2O$, EMSURE® ACS) were used as-received for the fabrication processes of BC and BC/$MnFe_2O_4$ nanocomposite membranes.

2.2 Bacterial Cellulose Cultivation

Komagataeibacter xylinus DSM 2325 (DSMZ, Germany) was streak-plated on Hestrin-Schramm (HS) agar (g/L: peptone, 5; yeast extract, 5; disodium hydrogen phosphate, 2.7 and citric acid, 1.15, supplemented with 2% glucose and 0.2 % cellulase) from glycerol stocks and incubated at 30 °C for 3 days. Single colonies from HS agar were inoculated in 5 ml of glucose yeast extract (GYE) medium (consisting of 50 g D-glucose (dextrose) anhydrous and 5 g yeast extract in 1 L of MQ water) for 3 days at 30 °C with agitation at 180 rpm. This produced actively growing cells that were transferred into 45 ml of GYE medium and allowed to grow under the same conditions, producing a starter culture. For fabrication of BC sheets, the cells were transferred into a GYE medium without cellulase at a ratio of 1 ml cells: 45 ml GYE medium. Cells were cultivated at 30 °C under a static condition for 10 days in 6-cm round-shaped Petri dishes. After that, BC hydrogels were harvested, washed in boiling water for 1 h and immersed in 0.5 M NaOH and 5 wt% NaOH for 15 min and 24 h, respectively. Next, the BC hydrogel was washed by DI water several times to remove the medium and the alkali solution until it reached a neutral pH. The BC hydrogels harvested at this stage were around 0.4 cm thick and and 6.0 cm in diameter. The BC hydrogels were either dried by hot-pressing at 60 °C for 8 h to obtain flat BC films or used in their wet state as a template for the synthesis of BC/$MnFe_2O_4$ nanocomposites.

2.3 Synthesis of BC/$MnFe_2O_4$ Nanocomposites

BC/$MnFe_2O_4$ nanocomposites were prepared via a co-precipitation method of $MnFe_2O_4$ nanoparticles in the presence of BC hydrogels. First, 0.05 M $FeCl_3.6H_2O$ and 0.025 M $MnCl_2.4H_2O$ were dissolved in DI water, and then the BC hydrogels were immersed in the solution for 15 min. The solution containing the BC hydrogels was heated to 65 °C and held at this temperature for 4 h. At this stage, the color of the BC hydrogels changed from clear white

to orange, indicating the anchoring process of the metallic ions (Mn^{2+}, Fe^{3+}) on the surfaces of the BC nanofibrils. The samples were transferred into a NaOH solution (1.2 M) and kept at 65 °C for 4 h, resulting in a reaction of metallic ions (Mn^{2+}, Fe^{3+}) to form $MnFe_2O_4$ according to the chemical reaction:

$$MnCl_2.4H_2O + 2FeCl_3.6H_2O + 8NaOH \rightarrow MnFe_2O_4 + 8NaCl + 14H_2O$$

During this process, the color of BC hydrogels changed rapidly from orange to black. The product was washed with DI water several times until a neutral pH was achieved. $MnFe_2O_4$ nanoparticles were homogeneously dispersed throughout the BC hydrogel (Fig. S1, Supplementary Information). Finally, they were dried by hot-pressing at 60 °C for 8 h to obtain flat BC/$MnFe_2O_4$ composite films. The fabrication processes are summarized in Fig. 1. The sample with manganese ferrite nanoparticles in the BC matrix (BC/$MnFe_2O_4$) is referred to as MBC in the remainder of the paper.

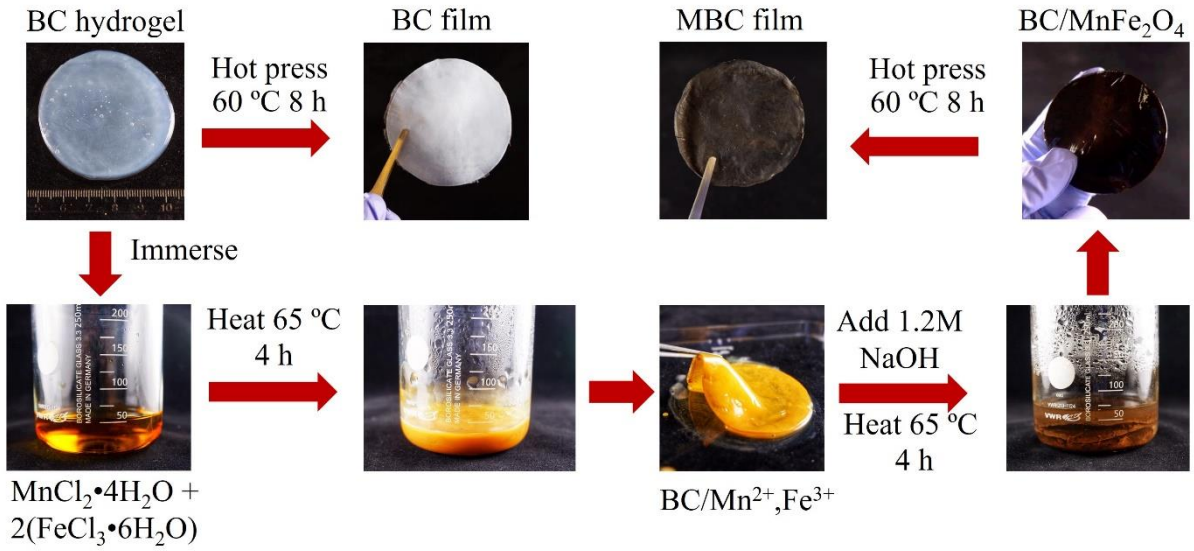

Fig. 1. Schematic for the fabrication processes of a BC film and BC/$MnFe_2O_4$ (MBC) nanocomposite film.

The amount of $MnFe_2O_4$ in the composite films was determined using a thermogravimetric analysis (TGA) technique (Hitachi, STA7200, Japan). As shown in Fig. S2 (Supplementary Information), the content of $MnFe_2O_4$ in the composites was around 27 wt.%. We varied the $MnFe_2O_4$ concentration and found that larger concentrations of $MnFe_2O_4$ produced higher piezoelectric sensitivity. However, at exceedingly high $MnFe_2O_4$ levels, the MBC composite film showed current leakage, and piezoelectric measurements could not be

done. This is probably due to the significantly higher electrical conductivity of $MnFe_2O_4$ (1.64 S m^{-1}) [30] than pristine BC (8.5×10^{-3} S m^{-1}) [31]). Thus, the amount of $MnFe_2O_4$ in this paper is at the maximum concentration possible that can be incorporated in the BC structure without short circuiting.

Additionally, for the measurement of piezoelectric sensitivity, the samples were sandwiched between two electrodes. Since current leakage was experienced in some cases, the film thickness was increased by stacking the films. Four different sample configurations were prepared as shown in Fig. 2. They are denoted as BC, MBC, BC/BC/BC and BC/MBC/BC based on composition. The effect of multilayered sheets on the piezoelectric response was investigated. We observed that the pristine BC film was more robust than the composite films. For this reason, we explored stacking of composite film and pristine BC films as depicted in Fig. 2d.

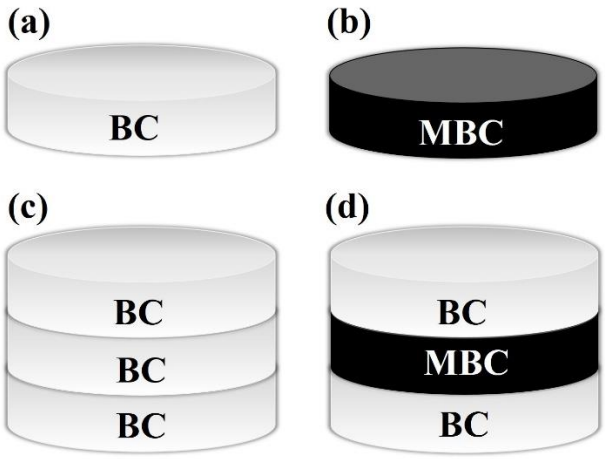

Fig. 2. Four different configurations of the samples for piezoelectric response measurement: (a) BC, (b) MBC, (c) BC/BC/BC, and (d) BC/MBC/BC.

2.4 Material Characterization

The surface and cross-sectional morphology of the films were characterized using scanning electron microscopy (FEI, Helios). Prior to SEM imaging, the samples were sputter-coated with a thin layer of gold to avoid electrical charging by the electron beam. The details of the cellulose fibers and nanoparticles were characterized using transmission electron microscopy (TEM, Thermo Scientific, Talos F200X). A small piece of the film was immersed in ethanol and ultrasonicated for 10 min. The solution was dropped on a holey carbon grid for TEM imaging. X-ray diffraction (XRD) patterns were measured employing Cu-Kα radiation

(PANalytical, Empyrean) to obtain information on the phases and crystalline structures. The patterns were recorded using a reflection mode in the 5–80° 2θ range. Atomic force microscopy (AFM, Park XE-100) was used to characterize the surface topography.

2.5 Electrode Fabrication and Piezoelectric Sensitivity Measurements

Electrodes were attached on both sides of the BC or BC nanocomposite films for measurement of piezoelectric sensitivity. Cu or carbon were selected as the electrode materials to investigate the effect of the electrode material on sensor performance. In the case of Cu, round-shaped 15 mm electrodes were produced by evaporating 100 nm of Cu onto a polyethylene terephthalate (PET) substrate through a laser-cut metallic stencil mask (Fig. 3a). BC or BC composite films were placed between the electrodes. For the carbon electrodes, 10 mm adhesive carbon tapes were attached on the surfaces of the films (Fig. 3b).

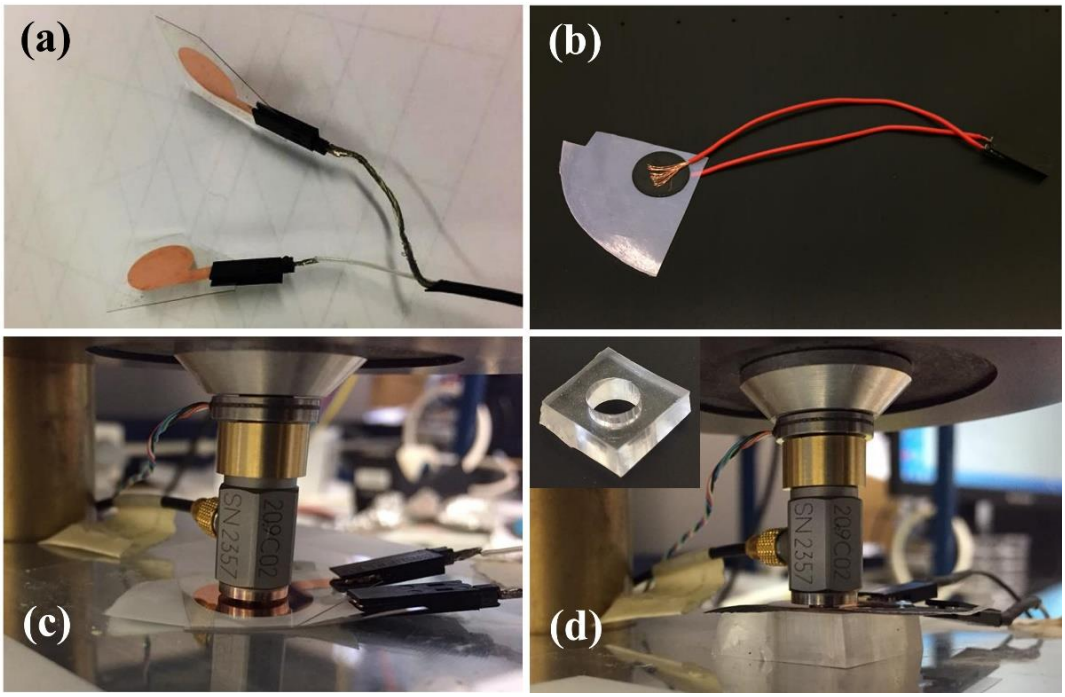

Fig. 3. (a) Cu electrodes on PET substrates, (b) carbon tape electrode attached to the film, (c) normal mode measurement setup, (d) bending mode measurement setup (inset: a PDMS ring).

Piezoelectric sensitivity was measured as previously described [15]. A schematic of the measurement setup is shown in Fig. S3a in the Supplementary Information. Briefly, the piezoelectric sensitivity measurements were conducted by generating a dynamic excitation force with a Type 4810 Mini-Shaker (Brüel & Kjær). A commercial high sensitivity dynamic

force sensor (PCB Piezotronics Model 209C02) and a load cell (Measurement Specialties Inc. Model ELFS-T3E-20L) were respectively used as reference sensors for the dynamic excitation force, and a reference sensor to measure the static force between the sample and shaker's piston. A 3 N applied static force was required to keep the sample in place and prevent the piston from leaving the sample surface during the measurement. A sinusoidal dynamic excitation force of 1.4 N with a constant frequency of 2 Hz was applied during measurements.

Piezoelectric sensitivity in the units of pC/N was determined by dividing the amplitude of the generated charge signal by the amplitude of applied dynamic force signal. The generated charge was measured using a charge amplifier and a 16-bit AD converter. Sinusoidal amplitude values were determined by fitting the sinusoidal charge and force signals. This is described in the IEEE Standard for Digitizing Waveform Recorders (IEEE Standard 1241). The measured sensitivity in the longitudinal direction is closely related to the piezoelectric d_{33} coefficient that describes electric polarization generated in the same direction as an applied force [32].

The piezoelectric responses were tested in both normal and bending modes. In the normal mode, force was applied perpendicular to the film (Fig. 3c). In the bending mode (Fig. 3d), a PDMS ring (inset of Fig. 3d) was inserted under the sample allowing the films to bend. The linear dependence of the piezoelectric sensitivity values on dynamic force was also studied as previously described [33]. The 2 Hz dynamic force was varied from 0.1 to 5.0 N, and the sensitivity measured. To increase the accuracy of the output data, five different excitation positions (Fig. S3b in the Supplementary Information) were used for the sensitivity measurements on each sample. Furthermore, three samples were used for each configuration described in Fig. 2. A PVDF film (Measurement Specialties Inc., USA; thickness 28 μm) with known piezoelectric properties was used as a reference material.

3. Results and discussion

3.1 BC and BC Nanocomposite Film Characterization

Fig. 4a shows an SEM image of the surface of a BC film. It consists of a three-dimensional network comprised of ultrafine cellulose fibrils with an average diameter of 104 ± 22 nm. However, the fibers seem blended due to inter-fibril bonding. For the composite sample, the three-dimensional network structure of BC remained unchanged after being loaded with $MnFe_2O_4$ nanoparticles. The $MnFe_2O_4$ nanoparticles are evenly distributed and robustly anchored on the surface of the nanofibrils as well as in the inter-nanofibrillar spaces (Fig. 4b). These nanoparticles could decrease the interaction between the nanofibrils and thus expand the

volume of the samples, which is evident from the greater thickness of the MBC (23 ± 1 μm) compared to the BC film (19 ± 1 μm).

The AFM topographical images of the BC and MBC films are shown in Fig. 4c and 4d, respectively. The topography of the BC presents densely packed nanofibers in random orientation. The average size of the fibers is 95 ± 22 nm, slightly smaller than the value measured in SEM imagery (104 ± 22 nm). This could have been due to the thin gold coating applied for SEM imaging. The maximum roughness of the BC surface is about 1 μm. The topographical surfaces of the MBC film were covered with $MnFe_2O_4$ nanoparticles. The features of BC nanofibers could not be visualized. AFM results confirm that a large proportion of $MnFe_2O_4$ nanoparticles were loaded into the MBC film.

The XRD patterns of the BC and MBC films are shown in Fig. 4e and 4f. The BC film presents diffraction peaks at 2θ values of 15.1°, 17.7°, and 23.5° that can be indexed as the $(1\bar{1}0)$, (110) and (200) planes for cellulose Iα [34]. On the other hand, the MBC film shows a diffraction peak at 23.5°, corresponding to the (200) plane of BC, and additional peaks at 30.0°, 35.2°, 42.7°, 56.4°, and 61.9°, corresponding to the primary diffraction of the (220), (311), (400), (511), and (440) planes of the $MnFe_2O_4$ phase. The $MnFe_2O_4$ phase diffraction peaks were indexed according to the standard reference (JCPDS No. 10-0319), and previous reports [35, 36]. XRD analysis, therefore, confirms the formation of composite phases in the MBC film.

TEM images of the MBC film are presented in Fig. 5. They show $MnFe_2O_4$ nanoparticles distributed evenly along the surfaces of the BC nanofibers. The $MnFe_2O_4$ nanoparticles are very small, with an average particle size of 3.6 ± 0.6 nm.

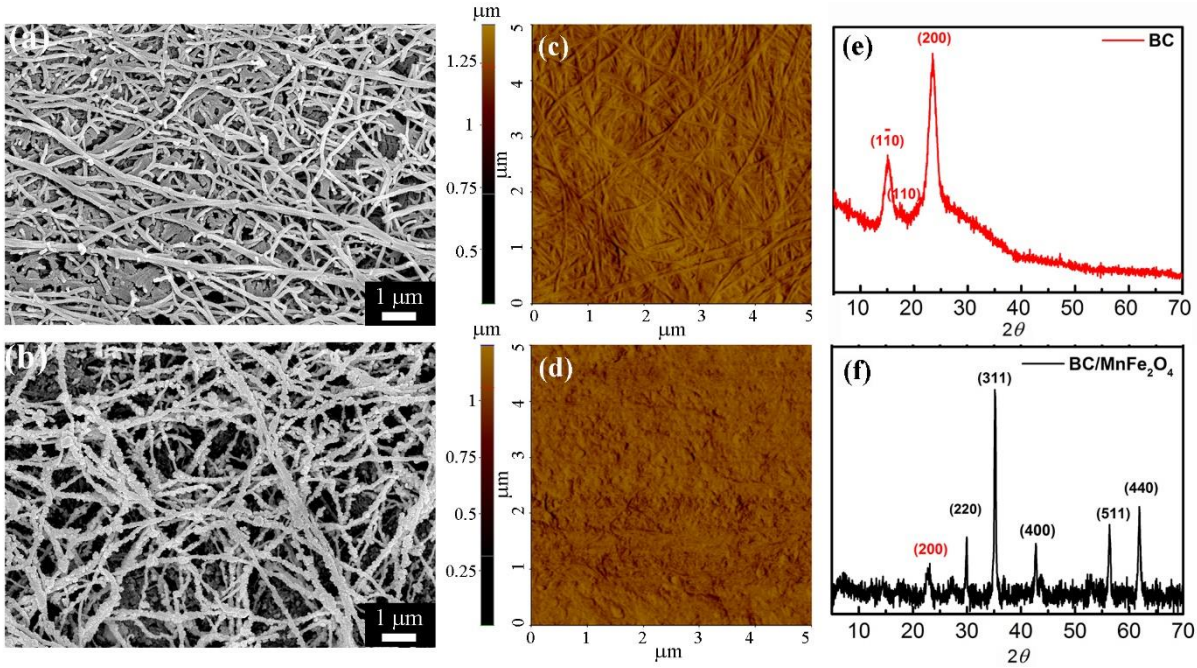

Fig. 4. Surface morphology of BC (a,c) and MBC (b,d) films using SEM and AFM analysis. (e) and (f) XRD patterns of BC and MBC films, respectively.

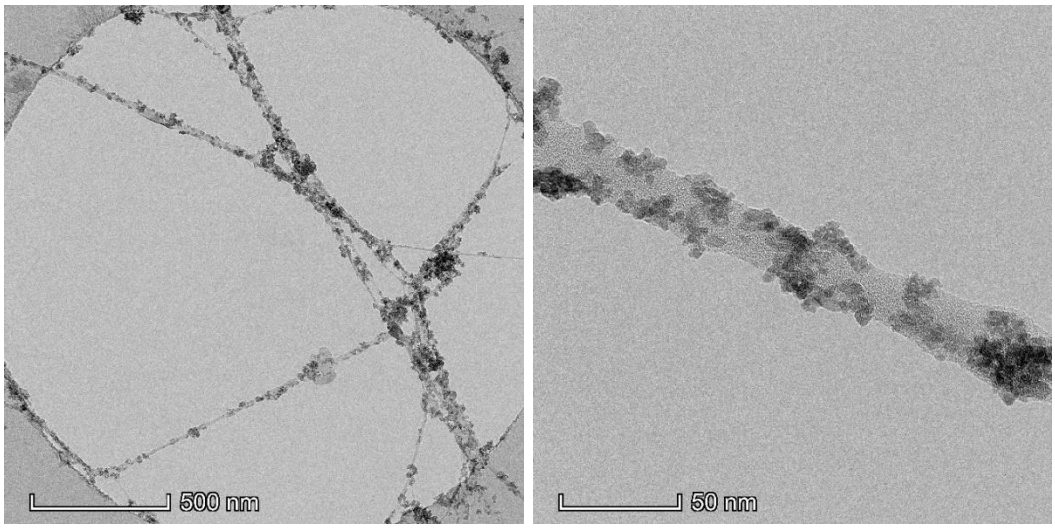

Fig. 5. TEM images of the MBC sample.

For the three-layer films, cross-sectional SEM images were made to observe the interfaces between the layers, as shown in Fig. 6. For the BC/BC/BC stacked layers (Fig. 6a), the inter-layer interfaces are difficult to observe, presumably due to strong interfibrillar bonding. Alternatively, the BC/MBC/BC film (Fig. 6b) distinctly shows the three layers and the interlayer interfaces can be visualized. The distinction could be possible to a difference in the fibril–fibril bonding between the BC layer and the MBC composite layer. The BC/MBC/BC

film is thicker (41 μm) than the BC/BC/BC film (35 μm), which could be a result of impregnation of $MnFe_2O_4$ nanoparticles into the BC nanostructure.

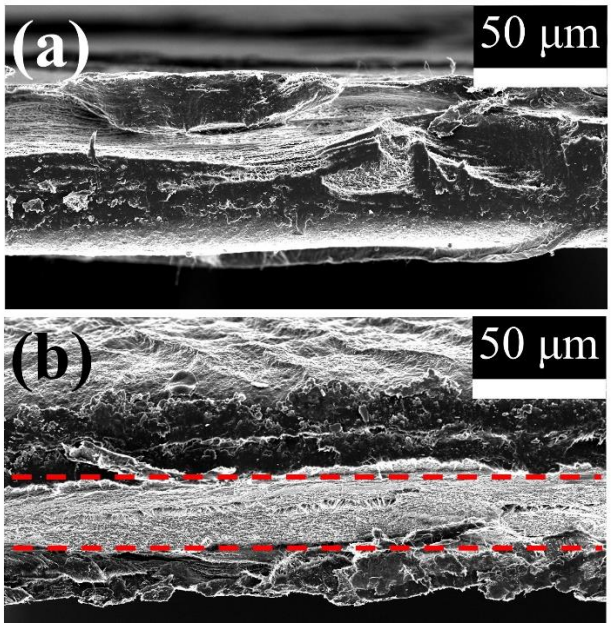

Fig. 6. Typical cross-sectional SEM images of (a) BC/BC/BC and (b) BC/MBC/BC films.

3.2 Piezoelectric Sensitivity Measurements

The piezoelectric sensitivities of the BC and MBC films using Cu electrodes are presented in Fig. 7. The values presented in the graphs are the average of five excitation positions. The variation amongst each sample (three pieces of the film) is small indicating the stability and reproducibility of the piezoelectric response. In the normal mode (Fig. 7a), the BC film shows a piezoelectric sensitivity of 4-5 pC/N, similar to a previous study [15]. The piezoelectric sensitivity increased substantially, reaching about 20-23 pC/N, for the MBC film. Incorporation of $MnFe_2O_4$ nanoparticles in the BC structure significantly improved the piezoelectric response of this film. The results showing the effect of multilayered sheets on the piezoelectric response are presented in Fig. 7a. It can be clearly seen that even though the three-layered films improved the robustness of the samples and prevented short circuits, they caused a decrease in the piezoelectric sensitivity. BC/BC/BC sheets possess a sensitivity of around 3 pC/N, slightly lower than that of a single BC sheet. Piezoelectric sensitivity of the BC/MBC/BC sheets ranged from 5-7 pC/N, much lower than the single MBC sheet. The reasons for the piezoelectric reduction for the BC/MBC/BC multilayered sheets could be due a change in the film thickness [37, 38]. Furthermore, the force per thickness decreased which caused decreased charge separation in the film. In the case of the BC/MBC/BC sample, poor bonding between layers could be one of the reasons for reduced piezoelectric sensitivity. A

possible approach to improve this is by treating the surface of BC prior to hot-pressing, or by using vacuum hot-pressing. Also, the charge separation in the MBC film does not affect the BC film on both side, and that causes decreased sensitivity.

In the bending mode (Fig. 7b), the piezoelectric sensitivity of all samples was improved compared to the normal mode. Sensitivity values are in the range of 22-25 pC/N and 51-57 pC/N for the BC and the MBC films, respectively. The enhanced piezoelectric sensitivity in the bending mode is due to the different mode of the applied force, so that the piezoelectric coefficients are also different in that mode. Furthermore, the BC and MBC films exhibit high flexibility in the bending mode leading to an improved piezoelectric response. On the other hand, the multilayered sheets show only a slight piezoelectric enhancement in the bending mode compared to the normal mode. Even though multilayering improved the mechanical robustness of films [39], it reduced the film flexibility, which is an important parameter for high piezoelectric sensitivity in the bending mode.

For comparison, the piezoelectric response of a commercial PVDF film was measured using the same setup. The sensitivity values were approximately 25 pC/N for the normal mode and 360 pC/N for the bending mode. It can be seen that the piezoelectric sensitivity of the MBC film is comparable to that of commercial PVDF in the normal mode, but still much lower in the bending mode. This could be due to the fabrication process of PVDF which involves voltage poling in combination with simultaneous lateral elongation, leading to a very high piezoelectric coefficient in the bending mode. We must emphasize that the BC and MBC films in this study were not subjected to intentional polarization or orientation as was the commercial stretched and poled PVDF film [40]. However, BC and MBC films have some natural orientation which results in significant piezoelectric responses. It is possible that the piezoelectric sensitivity of the MBC films could be further enhanced using proper poling.

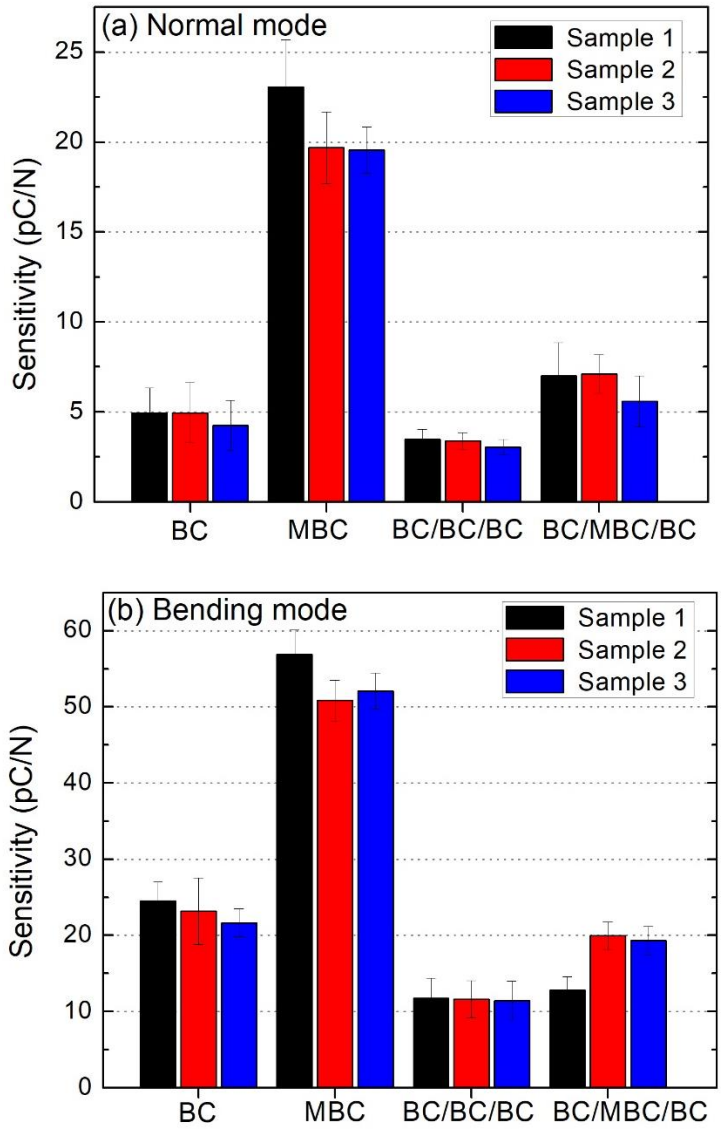

Fig. 7. Piezoelectric sensitivity of the BC and MBC films in the (a) normal mode and (b) bending mode.

In Fig. 7, evaporated Cu films on a PET substrate were used as electrodes, and the samples were sandwiched between them (Fig. 3a). Under this design, there could be poor electrical contact between the samples and the electrodes, resulting in a deteriorated piezoelectric response. To address the problem, we attached adhesive carbon tapes on the surfaces of the films (Fig. 3b), and used them as electrodes. The results, using carbon tape electrodes rather than Cu electrodes, are illustrated in Fig. 8. Several-fold improvement was observed. With carbon electrodes, the BC film exhibited a piezoelectric sensitivity of 10-16 pC/N whereas a sensitivity value greater than 50 pC/N was found for the MBC film. Moreover, the advantage of this design is not only for better contact, but the samples could be

used as stand-alone sensors. A sensitive and flexible piezoelectric device could be fabricated using the MBC film by simply attaching it to carbon tape.

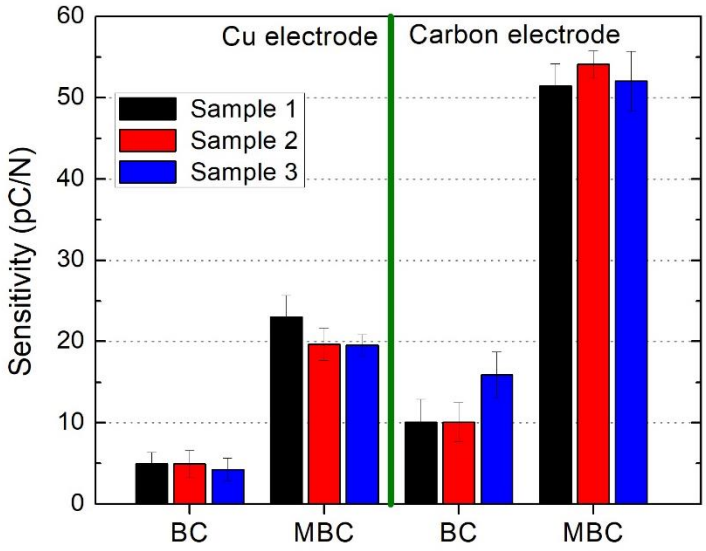

Fig. 8. Comparison of the piezoelectric sensitivity (normal mode) of the BC and MBC films using Cu or carbon electrodes.

The linearity of the piezoelectric response of the BC and MBC films was further studied by increasing dynamic excitation force applied to the films (using Cu electrodes). As shown in Fig. 9, the sensitivity of every sample increased as a function of the applied force in both normal and bending modes. The sensitivity is highest for the MBC film, reaching 80 pC/N in both modes, at a maximum force of 5 N. However, some nonlinearity can be observed in the signal from all films. The nonlinearity is determined using a least-square fit to a first degree polynomial. Instead of showing the maximum deviation from a linear transfer function [41], the nonlinearity presented in Table S1 (Supplementary Information) is expressed as the mean ± standard deviation of data point deviations from the fitted polynomial [33, 42]. The nonlinearity was found to be 2.73 ± 1.51 pC/N and 2.05 ± 1.27 pC/N for the MBC film measured in the normal and bending modes, respectively.

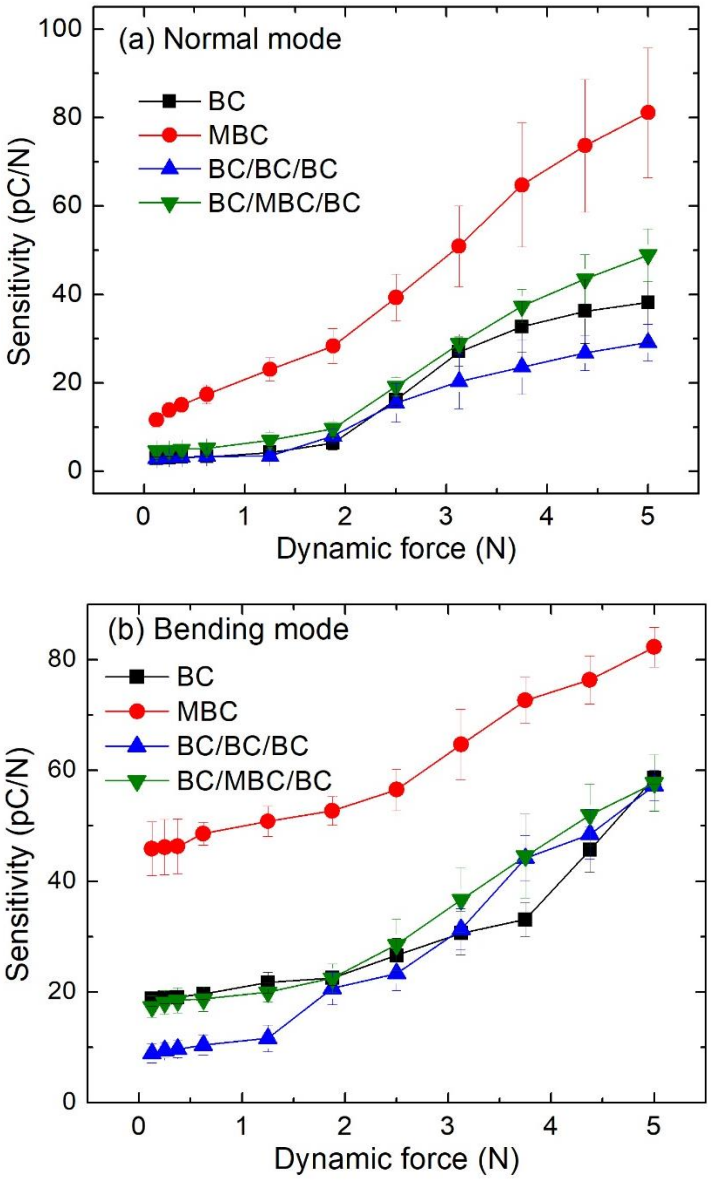

Fig. 9. Piezoelectric response of BC and BC composite films under increased mechanical loads in the (a) normal mode and (b) bending mode.

Our experiment demonstrated that by incorporating $MnFe_2O_4$ nanoparticles into the BC nanostructure, the piezoelectric sensitivity was considerably enhanced. The sensitivity of the MBC film was greater than 20 pC/N in the normal mode (Fig. 7a) and was enhanced to more than 50 pC/N when carbon tape was employed as electrodes (Fig. 8). The MBC sensor showed an almost linear response with increasing dynamic force (Fig. 9). In comparison to other nanocellulose-based piezoelectric films, our sensors have comparable performance and in some cases their performance was superior. For pristine nanocellulose films, a piezoelectric sensor based on wood nanocellulose fibers exhibited a sensitivity of approximately 5 pC/N [42]. In the case of the composite cellulose films, the piezoelectric sensitivity of nanocellulose

and chitosan-based films were found to be less than 10 pC/N [43]. Mahadeva et al. fabricated piezoelectric paper from wood cellulose fibers with d_{33} < 1 pC/N [44]. The sensitivity increased to 5 pC/N for cellulose fibers composited with $BaTiO_3$ [44]. In another study, hybrid paper with a large piezoelectric coefficient (d_{33} of 37-45 pC/N) was fabricated from wood nanocellulose mixed with $BaTiO_3$ and carboxymethylcellulose (CMC) [45]. Recently, a nanocellulose-based piezoelectric nanogenerator was developed [46-48]. With the addition of $BaTiO_3$ nanoparticles, both the voltage and current outputs increased with the $BaTiO_3$ content [46-48]. However, the piezoelectric sensitivity (d_{33}) was not reported, so it is difficult to make a direct comparison to our current research.

In our previous paper [15], values from 5 to 15 pC/N were obtained for pristine BC films, which were fabricated using various bacterial strains. In this work, we obtained a sensitivity of about 5 pC/N for pristine BC films, which corresponds well with the results of our previous work using pristine BC films prepared from the same bacterial strain. In addition to the BC film type, some variance in the sensor output was observed depending on the location of sensor electrodes on the same BC-sheet in both the curent and previous papers. Furthermore, we observed that the use of carbon tape electrodes instead of sandwiched Cu-electrodes produces 2-3 times greater measured sensitivity for both BC and MBC film types. We suggest that this results arises from better contact provided by the carbon tape between the electrodes and the sensor film. This enables better electrical transport into the charge amplifier connected to the sensor output.

The mechanism for enhancing piezoelectricity by the addition of $MnFe_2O_4$ nanoparticles in BC is not clear at present. In the case of the $BaTiO_3$-nanocellulose system, the piezoelectric enhancement was mostly due to the large piezoelectric coefficient of $BaTiO_3$ (d_{33} ~191 pC/N) [47]. In our case, $MnFe_2O_4$ is not known for its piezoelectricity and alternative explanations are required. Gonçalves et al. studied the magnetoelectric properties of PVDF/$CoFe_2O_4$ composites [49]. The piezoelectric coefficient of their composites increased with the $CoFe_2O_4$ content due to strong interfacial interactions between particles and the polymer matrix. The interfacial elastic effect was stronger leading to a higher piezoelectric response [49, 50]. Since $MnFe_2O_4$ is in the same family as $CoFe_2O_4$ (sharing the same crystal structure), this could be one of the possible reasons. Furthermore, Behera and Choudhary studied multiferroic characteristics of PVDF/$MnFe_2O_4$ nanocomposites [51]. They explained that the piezoelectric properties of the composite were improved due to strong electrostatic interaction and coupling between the $MnFe_2O_4$ nanoparticles and polymer at the interface

region [51, 52]. The transduction properties were hence improved. Alternatively, the improved piezoelectric response in our MBC film could be attributed to a reduced absorption of the applied stress by the BC fiber network, and also a more effective transfer of strain due to the presence of nanoparticles [45]. Nevertheless, further experiments are necessary for a deeper understanding of these phenomena.

4. Conclusions

We fabricated a BC/$MnFe_2O_4$ composite film with enhanced piezoelectric properties. $MnFe_2O_4$ nanoparticles were easily incorporated in a BC nanostructure via a co-precipitation process. The presence of BC and $MnFe_2O_4$ phases in the composite films were confirmed using SEM, AFM, TEM and XRD. The piezoelectric sensitivity measurements showed that the sensitivity of the MBC film was improved by about 4-5 times in the normal mode over that of a pristine BC film. In the bending mode measurements, MBC exhibited a sensitivity of 51-57 pC/N, about 2-3 times greater than its pure BC counterpart. The underlying mechanism for the enhanced piezoelectric response for the composite film is not absolutely clear, but it is most likely due to strong interfacial interactions between the nanoparticles and polymer, and/or a more effective transfer of the strain due to the presence of nanoparticles. Furthermore, the MBC composite film demonstrated an almost linear dependence of the piezoelectric response and applied force, with a maximum value of 80 pC/N at a dynamically applied force of 5 N. Additionally, the piezoelectric response was significantly enhanced when carbon tape was used as electrodes. Therefore, a simple design of MBC film with carbon tape electrodes can be potentially used as a stand-alone piezoelectric sensor with high flexibility and sensitivity. This type of low-cost and environmentally friendly piezoelectric sensor is suitable for physiological sensors, such as feet pressure measurements or heart rate monitoring, or use in Internet-of-Things sensor tag applications where disposable sensors are desirable.

Acknowledgements

This work was supported by the Thailand Research Fund (TRF) in cooperation with the Synchrotron Light Research Institute (public organization) and Khon Kaen University (RSA6280020), the Royal Golden Jubilee PhD Programme (PHD/0063/2558), and the Research Network NANOTEC (RNN) program of the National Nanotechnology Center (NANOTEC), NSTDA, Ministry of Higher Education, Science, Research and Innovation, and Khon Kaen University.

References

1. Curie, P. and P. Curie, Crystal Physics: Development by Pressure of Polar Electricity in Hemihedral Crystals with Inclined Faces, 1880. **91**: p. 294.
2. Lee, H.J. and S.M. Arnold, *Smart Materials, Precision Sensors/Actuators, Smart Structures, and Structronic Systems AU - TZOU, H. S.* Mechanics of Advanced Materials and Structures, 2004. **11**(4-5): p. 367-393.
3. Gupta, V., M. Sharma, and N. Thakur, *Optimization Criteria for Optimal Placement of Piezoelectric Sensors and Actuators on a Smart Structure: A Technical Review.* Journal of Intelligent Material Systems and Structures, 2010. **21**(12): p. 1227-1243.
4. May, E.L., *Application of a piezoelectric sensor for measuring shivering in a small marsupial.* Journal of Thermal Biology, 2003. **28**(6): p. 469-475.
5. Nguyen, Q., et al., *Characteristics of an Insect-mimicking Flapping System Actuated by a Unimorph Piezoceramic Actuator*. Vol. 19. 2008. 1185-1193.
6. Schlaberg, H.I. and J.S. Duffy, *Piezoelectric polymer composite arrays for ultrasonic medical imaging applications.* Sensors and Actuators A: Physical, 1994. **44**(2): p. 111-117.
7. Terry, S., et al., *Silicon pressure transducer arrays for blood-pressure measurement.* Sensors and Actuators A: Physical, 1990. **23**(1): p. 1070-1079.
8. Lee, H.S., et al., *Flexible Inorganic Piezoelectric Acoustic Nanosensors for Biomimetic Artificial Hair Cells.* Advanced Functional Materials, 2014. **24**(44): p. 6914-6921.
9. Akdogan, E.K., M. Allahverdi, and A. Safari, *Piezoelectric composites for sensor and actuator applications.* IEEE Transactions on Ultrasonics, Ferroelectrics, and Frequency Control, 2005. **52**(5): p. 746-775.
10. Chen, Q.X. and P.A. Payne, *Industrial applications of piezoelectric polymer transducers.* Measurement Science and Technology, 1995. **6**(3): p. 249-267.
11. Tressler, J.F., et al., *Functional composites for sensors, actuators and transducers.* Composites Part A: Applied Science and Manufacturing, 1999. **30**(4): p. 477-482.
12. Martins, P., A.C. Lopes, and S. Lanceros-Mendez, *Electroactive phases of poly(vinylidene fluoride): Determination, processing and applications.* Progress in Polymer Science, 2014. **39**(4): p. 683-706.
13. Lee, S., et al., *Multifunctional Flexible Device Based on Phosphor on Piezoelectric Polymer: Lighting, Speaking, and Pressure-Light Converting.* physica status solidi (a), 2018. **215**(13): p. 1701071.
14. Persano, L., et al., *High performance piezoelectric devices based on aligned arrays of nanofibers of poly(vinylidenefluoride-co-trifluoroethylene).* Nature Communications, 2013. **4**: p. 1633.
15. Mangayil, R., et al., *Engineering and Characterization of Bacterial Nanocellulose Films as Low Cost and Flexible Sensor Material.* ACS Applied Materials & Interfaces, 2017. **9**(22): p. 19048-19056.
16. Dargaville, T.R., M. Celina, and P.M. Chaplya, *Evaluation of piezoelectric poly(vinylidene fluoride) polymers for use in space environments. I. Temperature limitations.* Journal of Polymer Science Part B: Polymer Physics, 2005. **43**(11): p. 1310-1320.
17. Curry, E.J., et al., *Biodegradable Piezoelectric Force Sensor.* Proceedings of the National Academy of Sciences, 2018. **115**(5): p. 909-914.
18. Pirich, C.L., et al., *Piezoelectric immunochip coated with thin films of bacterial cellulose nanocrystals for dengue detection.* Biosensors and Bioelectronics, 2017. **92**: p. 47-53.
19. Zhang, G., et al., *Uniformly assembled vanadium doped ZnO microflowers/ bacterial cellulose hybrid paper for flexible piezoelectric nanogenerators and self-powered sensors.* Nano Energy, 2018. **52**: p. 501-509.
20. Doaga, A., et al., *Synthesis and characterizations of manganese ferrites for hyperthermia applications.* Materials Chemistry and Physics, 2013. **143**(1): p. 305-310.
21. Sahoo, B., et al., *Biocompatible mesoporous silica-coated superparamagnetic manganese ferrite nanoparticles for targeted drug delivery and MR imaging applications.* Journal of Colloid and Interface Science, 2014. **431**: p. 31-41.

22. Guo, P., et al., *Electrochemical properties of colloidal nanocrystal assemblies of manganese ferrite as the electrode materials for supercapacitors.* Journal of Materials Science, 2017. **52**(9): p. 5359-5365.
23. Zhang, Z., et al., *Facile solvothermal synthesis of mesoporous manganese ferrite (MnFe2O4) microspheres as anode materials for lithium-ion batteries.* Journal of Colloid and Interface Science, 2013. **398**: p. 185-192.
24. Verma, K.C., et al., *Multiferroic effects in MFe2O4/BaTiO3 (M = Mn, Co, Ni, Zn) nanocomposites.* Journal of Alloys and Compounds, 2017. **709**: p. 344-355.
25. Fragouli, D., et al., *Superparamagnetic cellulose fiber networks via nanocomposite functionalization.* Journal of Materials Chemistry, 2012. **22**(4): p. 1662-1666.
26. Wang, H., et al., *Ultrafine Mn ferrite by anchoring in a cellulose framework for efficient toxic ions capture and fast water/oil separation.* Carbohydrate Polymers, 2018. **196**: p. 117-125.
27. Zhan, Y., et al., *Magnetic recoverable MnFe2O4/cellulose nanocrystal composites as an efficient catalyst for decomposition of methylene blue.* Industrial Crops and Products, 2018. **122**: p. 422-429.
28. Walanda, D.K., G.A. Lawrance, and S.W. Donne, *Hydrothermal MnO2: synthesis, structure, morphology and discharge performance.* Journal of Power Sources, 2005. **139**(1): p. 325-341.
29. Carta, D., et al., *A Structural and Magnetic Investigation of the Inversion Degree in Ferrite Nanocrystals MFe2O4 (M = Mn, Co, Ni).* The Journal of Physical Chemistry C, 2009. **113**(20): p. 8606-8615.
30. Cai, W., et al., *A facile approach to fabricate flexible all-solid-state supercapacitors based on MnFe2O4/graphene hybrids.* Journal of Power Sources, 2014. **255**: p. 170-178.
31. Dhar, P., et al., *Valorization of sugarcane straw to produce highly conductive bacterial cellulose / graphene nanocomposite films through in situ fermentation: Kinetic analysis and property evaluation.* Journal of Cleaner Production, 2019. **238**: p. 117859.
32. Ramadan, K.S., D. Sameoto, and S. Evoy, *A review of piezoelectric polymers as functional materials for electromechanical transducers.* Smart Materials and Structures, 2014. **23**(3): p. 033001.
33. Rajala, S., S. Tuukkanen, and J. Halttunen, *Characteristics of Piezoelectric Polymer Film Sensors With Solution-Processable Graphene-Based Electrode Materials.* IEEE Sensors Journal, 2015. **15**(6): p. 3102-3109.
34. Czaja, W., D. Romanovicz, and R.m. Brown, *Structural investigations of microbial cellulose produced in stationary and agitated culture.* Cellulose, 2004. **11**(3): p. 403-411.
35. Zhang, X.-J., et al., *Enhanced Microwave Absorption Property of Reduced Graphene Oxide (RGO)-MnFe2O4 Nanocomposites and Polyvinylidene Fluoride.* ACS Applied Materials & Interfaces, 2014. **6**(10): p. 7471-7478.
36. Wang, Y., et al., *Synthesis and Characterization of Single-Crystalline MnFe2O4 Ferrite Nanocrystals and Their Possible Application in Water Treatment.* European Journal of Inorganic Chemistry, 2011. **2011**(19): p. 2942-2947.
37. Cardoso, V.F., G. Minas, and S. Lanceros-Méndez, *Multilayer spin-coating deposition of poly(vinylidene fluoride) films for controlling thickness and piezoelectric response.* Sensors and Actuators A: Physical, 2013. **192**: p. 76-80.
38. Qaiss, A., et al., *Theoretical modeling and experiments on the piezoelectric coefficient in cellular polymer films.* Polymer Engineering & Science, 2013. **53**(1): p. 105-111.
39. Sriplai, N., et al., *White magnetic paper based on a bacterial cellulose nanocomposite.* Journal of Materials Chemistry C, 2018. **6**(42): p. 11427-11435.
40. Pörhönen, J., et al., *Flexible Piezoelectric Energy Harvesting Circuit With Printable Supercapacitor and Diodes.* IEEE Transactions on Electron Devices, 2014. **61**(9): p. 3303-3308.
41. Fraden, J., *Handbook of modern sensors: physics, designs, and applications*. 2010: Springer-Verlag New York. XV, 663.
42. Rajala, S., et al., *Cellulose Nanofibril Film as a Piezoelectric Sensor Material.* ACS Applied Materials & Interfaces, 2016. **8**(24): p. 15607-15614.
43. Hänninen, A., et al., *Nanocellulose and chitosan based films as low cost, green piezoelectric materials.* Carbohydrate Polymers, 2018. **202**: p. 418-424.

44. Mahadeva, S.K., K. Walus, and B. Stoeber, *Piezoelectric Paper Fabricated via Nanostructured Barium Titanate Functionalization of Wood Cellulose Fibers.* ACS Applied Materials & Interfaces, 2014. **6**(10): p. 7547-7553.
45. Mahadeva, S.K., K. Walus, and B. Stoeber, *Flexible and robust hybrid paper with a large piezoelectric coefficient.* Journal of Materials Chemistry C, 2016. **4**(7): p. 1448-1453.
46. Shi, K., et al., *Cellulose/BaTiO3 aerogel paper based flexible piezoelectric nanogenerators and the electric coupling with triboelectricity.* Nano Energy, 2019. **57**: p. 450-458.
47. Choi, H.Y. and Y.G. Jeong, *Microstructures and piezoelectric performance of eco-friendly composite films based on nanocellulose and barium titanate nanoparticle.* Composites Part B: Engineering, 2019. **168**: p. 58-65.
48. Zhang, G., et al., *Novel Piezoelectric Paper Based Flexible Nanogenerators Composed of BaTiO 3 Nanoparticles and Bacterial Cellulose*. Vol. 3. 2015. n/a-n/a.
49. Gonçalves, R., et al., *Development of magnetoelectric CoFe2O4 /poly(vinylidene fluoride) microspheres.* RSC Advances, 2015. **5**(45): p. 35852-35857.
50. Liu, X., et al., *Magnetoelectricity in CoFe2O4 nanocrystal-P(VDF-HFP) thin films.* Nanoscale Research Letters, 2013. **8**(1): p. 374.
51. Behera, C. and R.N.P. Choudhary, *Electrical and multiferroic characteristics of PVDF-MnFe2O4 nanocomposites.* Journal of Alloys and Compounds, 2017. **727**: p. 851-862.
52. Martins, P., et al., *Tailored Magnetic and Magnetoelectric Responses of Polymer-Based Composites.* ACS Applied Materials & Interfaces, 2015. **7**(27): p. 15017-15022.